Chemical Physics Letters 639 (2015) 131–134

Contents lists available at ScienceDirect

Chemical Physics Letters

journal homepage: www.elsevier.com/locate/cplett

# More aromatic molecular junction has lower conductance

Zhen Xie [a], Xiao-Li Ji [a], Yang Song [a,*], Ming-Zhi Wei [a,b], Chuan-Kui Wang [a,*]

[a] College of Physics and Electronics, Shandong Normal University, Jinan 250014, China
[b] School of Materials Science and Engineering, QiLu University of Technology, Jinan 250353, China

ARTICLE INFO

*Article history:*
Received 14 July 2015
In final form 8 September 2015
Available online 14 September 2015

ABSTRACT

The conductance of molecular junctions containing one of five-atom cyclic unit cyclopentadiene, furan, and thiophene sandwiched between two gold electrodes is theoretically investigated. It shows that when the molecules are adsorbed on pyramidal protruding or single atom protruding electrode surfaces, the conductance of these junctions show a negative relationship with their aromaticity, which is consistent with the experimental finding [34]. The analysis of the transmission coefficients and the molecular projected self-consistent Hamiltonian attributes this to the aromaticity dependent alignment of frontier molecular orbitals with the Fermi energy of electrodes.



## 1. Introduction

Understanding and controlling charge transport properties through molecular junctions has always been a formidable challenge in molecular electronics. Since molecular diode was first proposed in 1974 [1], molecular devices, such as molecular wires [2–4], molecular switches [5–7], nano rectifiers [8–10] and sensors [11–13], have been well developed. Theoretical and experimental work has revealed that the electron transport properties of molecular junctions can be influenced by either internal or external elements. It is demonstrated that tunneling distance [14–16], molecular conformation [17–19], contact configuration [20,21], coupling energy [22,23], HOMO-LUMO gap [9,24], and spatial distribution of orbitals [25–27] could effectively affect electron transport of molecular junctions. Meanwhile, some external modulations, such as protonation, light, external forces, also have been proved to be efficient methods to control the electron transport properties [28–32].

Recently, a series of experimental work has measured the conductance of single-molecule junctions created with aromatic rings using the scanning tunneling microscope-based break-junction (STM-BJ) technique [33,34]. A direct correlation between conductance and aromatic character of the molecular wires was focused. Measurements of conductance in single-molecule junction through diaminoacenes have shown that, for 1,4-diaminobenzene, 1,4-diaminonaphthalene, and 9,10-diaminoanthracene, the conductance increases with increasing number of benzo rings perpendicular to the transport direction [33]. The aromatic stabilizations of benzene, naphthalene, and anthracene were analyzed, and a negative correlation between conductance and aromaticity seemed to be obtained there [33]. However, because numbers of electrons in the π-systems of these acenes were different, a direct correlation between conductance and aromaticity was not determined. To further explore the correlation between aromaticity and conductance, Chen et al. have more recently measured the conductance of three single-molecule junctions containing one of five-atom cyclic units, nonaromatic cyclopentadiene derivative (⏢), aromatic furan (⏢), or the most aromatic thiophene (⏢), as shown in Figure 1 [34]. They found that the nonaromatic cyclopentadiene derivative was a better conductor than the aromatic furan junction, which was a better conductor than the most aromatic thiophene one, indicating a direct negative correlation between conductance and aromaticity. A qualitative elucidation for this finding was that a quinoid structure with the best conductance is more easily formed by compounds having lower initial aromatic stabilization, *i.e.*, the cyclopentadiene derivative herein [35].

In principle, as molecules have more aromatic character, their typical molecular orbitals would be more delocalized, which would be in favor of increasing conductance. However, Chen's experimental work presented an inverse and counterintuitive result. Therefore, whether this experimental finding is fabrication-scheme-dependent or not needs to be further clarified. In this work, we construct two series of single-molecule junctions with one of cyclopentadiene, furan and thiophene by varying molecule–electrode contact configurations, and then calculate their currents using the nonequilibrium Green's function method combined with density functional theory. The contact configurations between molecule and electrode are modeled and focused on. It is demonstrated that the conductance of such three

* Corresponding authors.
*E-mail addresses:* sunnymojie@126.com (Y. Song), ckwang@sdnu.edu.cn (C.-K. Wang).

http://dx.doi.org/10.1016/j.cplett.2015.09.017
0009-2614/

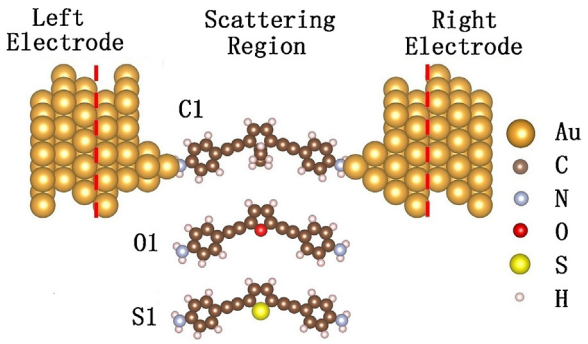


**Figure 1.** Schematic structures of molecular junctions with pyramidal protruding electrode surfaces. The molecules contain different cyclic five-membered rings: cyclopentadiene (C1), furan (O1), or thiophene (S1).

molecular wires is negatively associated with their aromaticity for both molecule–electrode contact configurations considered, which agrees with the Chen's experimental findings [34]. And it is revealed that this is due to variation of alignments between the frontier molecular orbital and the Fermi energy of electrodes due to different aromaticity of the molecule.

## 2. Theoretical model and computational details

A schematic illustration of the molecule junctions is displayed in Figure 1 Three different aromatic molecules, only differing in the central cyclic unit cyclopentadiene, furan, and thiophene, anchored with identical amino groups between two Au(1 1 1) surfaces are investigated. The computational model is divided into three regions, a left electrode, a central scattering region, and a right electrode. The central scattering region includes the target molecule and two Au surface layers at each side, where the screening effects are all taken into account. Each semi-infinite gold electrode is simulated by a $3 \times 4 \times 3$ unit cell by ways of using periodic boundary conditions. In order to calculate electronic structures of the electrode numerically, the Brillouin zone is sampled with a $4 \times 4 \times 10$ $k$-point grid using Monkhorst Pack scheme.

Geometric structures of the junctions are first optimized in the SIESTA code [36]. A protruding Au (1 1 1) surface contact configuration is proposed here to simulate the experimental conditions with STM-BJ technique [21,37,38], in which the three molecules are attached to protruding Au(1 1 1) surfaces laterally. During this optimization, the relative positions of the Au atoms on each side are frozen, but the distance between two Au clusters is relaxed along the $z$-axis (namely the transport direction). And all of the atoms in the bare molecule are relaxed until each component of the force on atom is less than 0.03 nN (0.02 eV/Å). Numerical atomic orbitals are employed as the basis set, and the core electrons are represented by Troullier–Martin-type norm-conserving pseudopotentials for the computation [39]. To reduce the computational cost but keep the accuracy, a single-ζ plus single polarization (SZP) basis set is employed for Au atoms and a double-ζ plus single polarization (DZP) basis set for the other atoms. The Perdew–Burke–Ernzerhof (PBE) exchange-correlation functional is adopted for the generated gradient approximation (GGA) [40]. An energy shift parameter of 100 meV is used for generating the cutoff radii of the pseudoatomic orbitals, and a 300 Ry mesh cutoff is set for the grid sampling to achieve a balance between the computing time and the accuracy. The convergent criterion for the density matrix is chosen as $10^{-4}$.

Then the corresponding electronic transport properties of the junctions are studied subsequently in the TranSIESTA module [41]. Since the convergence of the transmission spectrum with respect to the $k$-point sampling is much slower than the one for the density matrix, a $20 \times 20$ $k$-point grid is used to get a well-converged transmission spectrum. The current through the junctions is calculated by the Landauer–Büttiker formula, which is written as, $I = \frac{2e}{h} \int T(E,V)[f(E-\mu_L) - f(E-\mu_R)]dE$, where $T(E,V)$ is the bias-dependent electron transmission spectrum defined as $T(E,V) = Tr[\Gamma_L G_M \Gamma_R G_M^{\dagger}]$, $G_M$ the retarded Green's function of the extended molecule, $\Gamma_{L(R)}$ the coupling matrix between the scattering region and the left (right) electrode, $f$ the Fermi-Dirac distribution function and $\mu_{L(R)}$ is the electrochemical potential of the left (right) electrode.

## 3. Results and discussion

Considering the experimental fabrication scheme using STM-BJ technique to measure the conductance, we model the molecule–electrode contact configuration as a pyramidal protruding structure. The optimized structures of cyclopentadiene (C1), furan (O1) and thiophene (S1) with pyramidal protruding configurations are displayed in Figure 1. The three molecular junctions have extremely similar geometry, where the ending nitrogen atoms of each molecule are connected with the protruding Au atoms. Because the sulfur atom in the central five-membered ring has the largest size compared to the carbon and oxygen atoms, the molecule S1 has the largest intersection angle of 149° between the two acetylene bridges in the molecular backbone, and the longest molecular length of 2.0 nm accordingly. In these cases, the optimized results show that the molecule is absorbed laterally on the top Au atom of protruded pyramidal gold cluster by nitrogen atoms. Therefore, the main plane of central molecular backbone is vertical to the electrode surfaces in all the junctions, and the charge transport direction is then along $z$ axis.

In Figure 2(a), we present the current–voltage curves for C1, O1 and S1. It is found that the currents increase as bias voltages are enhanced. Most interestingly, for the three molecular junctions, one can see that the current values take an order of C1 > O1 > S1, which correlates negatively with the molecular aromaticity. This result demonstrates that the nonaromatic cyclopentadiene molecular junction has the highest conductance while the most aromatic of this series, thiophene one, has the lowest, showing a decreasing conductance due to molecular aromaticity enhancement. The simulation result has a good agreement with that observed in the experiment [34]. The calculated conductance at 0.2 V for these junctions are $6.1 \times 10^{-4}$ $G_0$, $3.9 \times 10^{-4}$ $G_0$, $3.7 \times 10^{-4}$ $G_0$ for C1, O1, and S1, respectively, where $G_0$ is the fundamental quantum of conductance $2e/h$. Here, we do not see a clear larger conductance as shown in the experimental finding [34] for furan derivative O1 when compared with that for the thiophene derivative S1. We attribute this to the molecule–electrode contact configuration effect on molecular energy level alignment with the Fermi energy of electrodes. And this will be unambiguously verified by a further atomic design of the molecule–electrode contact.

To understand the counterintuitively aromaticity enhancement induced decrease in the conductance, molecular orbital as well as transmission spectrum are analyzed and shown in Figure 2(b) and (c). The molecular eigenstates are investigated by diagonalizing the molecular projected self-consistent Hamiltonian (MPSH). In Figure 2(b), only the highest occupied molecular orbital (HOMO) and lowest unoccupied molecular orbital (LUMO) are presented. First, we find that the inset spatial distributions of HOMO and LUMO orbitals for three junctions are all well delocalized nearly independent on the aromaticity of the molecules. Also, the HOMO and LUMO energy levels do not change noticeably under external bias voltages, so that only these under zero bias voltage are given in Figure 2(b). This is because the whole junction is symmetric and at the same time both HOMO and LUMO orbitals locate outside the bias window [42]. In this term, the electron transport of these